LARGE EDDY SIMULATION TURBULENCE MODEL APPLIED TO FLOW OF NATURAL CONVECTION

Erica Pereira Carneiro

Dissertação de Mestrado apresentada ao Programa de Pós-graduação em Engenharia Civil, COPPE, da Universidade Federal do Rio de Janeiro, como parte dos requisitos necessários à obtenção do título de Mestre em Engenharia Civil.

Orientador: Fernando Luiz Bastos Ribeiro

Rio de Janeiro
Maio de 2015

LARGE EDDY SIMULATION TURBULENCE MODEL APPLIED TO FLOW OF NATURAL CONVECTION

Erica Pereira Carneiro

DISSERTAÇÃO SUBMETIDA AO CORPO DOCENTE DO INSTITUTO ALBERTO LUIZ COIMBRA DE PÓS-GRADUAÇÃO E PESQUISA DE ENGENHARIA (COPPE) DA UNIVERSIDADE FEDERAL DO RIO DE JANEIRO COMO PARTE DOS REQUISITOS NECESSÁRIOS À OBTENÇÃO DO GRAU DE MESTRE EM CIÊNCIAS EM ENGENHARIA CIVIL.

Examinada por:

Prof. Fernando Luiz Bastos Ribeiro, D.Sc.

Prof. Luiz Bevilacqua, D.Sc.

Prof. Augusto Cesar Noronha Rodrigues Galeão, D.Sc.

RIO DE JANEIRO, RJ - BRASIL

MAIO DE 2015

Carneiro, Erica Pereira

Large Eddy Simulation Turbulence Model Applied to Flow of Natural Convection / Erica Pereira Carneiro. - Rio de Janeiro: UFRJ/COPPE, 2015.

X, 37p.: il.; 29,7 cm.

Orientador: Fernando Luiz Bastos Ribeiro

Dissertação (Mestrado) - UFRJ/COPPE/Programa de Engenharia Civil, 2015.

Referências Bibilográficas: p. 36-37

1. Turbulência. 2. Equações de Navier-Stokes . 3. Modelo de Turbulência. 4. Implementação. I. Ribeiro, Fernando Luiz Bastos. II. Universidade Federal do Rio de Janeiro, COPPE, Programa de Engenharia Civil. III. Título.

Acknowledgments

I wish to express my sincere thanks to Fernando Luiz Bastos Ribeiro, Dean of the University and my master thesis advisor, for providing me with all the necessary facilities for the research and giving me the opportunity to explore such a fantastic topic.

I am also grateful to Henrique Conde Carvalho, my friend and co-advisor. I am extremely thankful and indebted to him for sharing expertise, sincere and valuable guidance and encouragement extended to me, without which the completion of this work would not be possible.

I would like to especially thank my two friends: Karyne Santos and Rodrigo Costa for their friendship and complicity. Without whom the daily life at the university was going to be very tedious.

I place on record, my sincere thanks to my friends: Nelson Santos, Mariane Rita, Renato Evangelista, Alfredo Flores, Rafaela Sanches, William Godoy and Vinicius Telles, who joined this venture with me since the beginning of my master studies.

I take this opportunity to express gratitude to all of the Department faculty members for their help and support.

I want to sincerely express my gratitude for my moms efforts to make every moment we spend together really unique.

I also thank my father and siblings for their unceasing encouragement, support and attention.

I would like to thank my friend, Aurea Florio, for her happiness!

To my best friend, Beatriz Carvalho, I would like to especially thank her for the support with all the sporting adventures!

I would like to express my sincere gratitude to the one that has been part of my journey for long, my husband and best friend Ricardo Lima, thanks for standing up for me whenever I needed and for being the one and only that soothes my heart.

I also place on record, my sense of gratitude to one and all, who directly or indirectly, have been part of this venture.

Erica Pereira Carneiro

May 2015

Resumo da Dissertação apresentada à COPPE/UFRJ como parte dos requisitos necessários para a obtenção do grau de Mestre em Ciências (M.Sc.)

MODELO DE TURBULÊNCIA LARGE EDDY SIMULATION APLICADO A FLUXO DE CONVECÇÃO NATURAL

Erica Pereira Carneiro

Maio/2015

Orientador: Fernando Luiz Bastos Ribeiro

Programa: Engenharia Civil

O presente trabalho apresenta a implementação de um modelo matemático de turbulência, usado em dinâmica dos fluidos computacional conhecido como Large Eddy Simulation (LES). A implementação é realizada em um modelo numérico bidimensional, baseado no Método dos Volumes Finitos (MVF) para a simulação de sistemas de escoamentos naturais com altas velocidades, isto é, com alto *Número de Reynolds (Re)*.

Abstract of Dissertation presented to COPPE/UFRJ as a partial fulfillment of the requirements for the degree of Master of Science (M.Sc.)

LARGE EDDY SIMULATION TURBULENCE MODEL APPLIED TO FLOW OF NATURAL CONVECTION

Erica Pereira Carneiro

May/2015

Advisor: Fernando Luiz Bastos Ribeiro

Department: Civil Engineering

This works presents an implementation of a mathematical model for turbulence used in computational fluid dynamics known as Large Eddy Simulation (LES). The implementation is performed in an existing bi-dimensional numerical model, based on the Finite Volume Method (FVM) for the simulation natural systems flows with high velocities, i.e., with high Reynolds Number (Re).

Contents

List of Figures

Chapter 1

Introduction

Most natural phenomena manifest themselves turbulently. Once fluids include gases, liquids and plasma, even our body can be an example of turbulent effects when thinking about blood flowing through our veins or air expanding in our lungs. Whenever we look around us it is possible to observe some turbulent manifestation. The rain falling, a river course, the wind flowing around us and so on. Rare are the phenomena that do not involve any manifestation of turbulence. One does not need to be a researcher or an expert to capture turbulent events, it is easy to delight ourselves in turbulence's unending variety of artistic forms. A first approach with the subject of turbulence, could make the phenomenon sound more like art than science. Since an elegant invitation is made by some researchers to think about it as the interplay of the two latter perspectives it is easy to concluded that one can enhance the other. As put by Leonardo da Vinci, "painting is a subtle *inventione* with which philosophy and subtle speculation considers the natures of all forms" and the contemporary science writer BALL (1999) wisely completed: "That's not a bad definition of science either, when you think about it". In the following figure it is possible to appreciate an interpretation of the phenomenon found in Leonardo da Vinci's sketch book followed by his description:

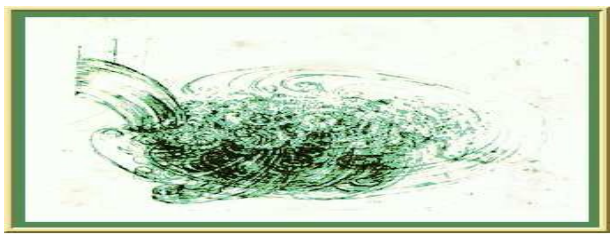

Figure 1.1: Da Vinci's sketch of turbulent flow

". . . the smallest eddies are almost numberless, and large things are rotated only by large eddies and not by small ones, and small things are turned by small eddies and large."

1.1 Brief History of Turbulence

The governing equations of fluid motion, first defined by EULER (1748), STOKES (1851) and NAVIER (1823), were the initial steps for the study and deepening of turbulence theory. Another important name and a remarkable collaboration for the study of the phenomenon was REYNOLDS (1883), whose pioneering work defined a quantity called the Reynolds number. A dimensionless critical number which expresses the balance between the nonlinear and dissipative properties of the flow and denotes the transition to turbulence. Later, PRANDTL (1963) made another attempt in understanding turbulence with his mixing length model. Reynolds work, from the 19th century, provided the foundation for HEISENBERG (1958)'s work (whose doctoral dissertation was entitled: "On the stability and turbulence of fluid flow"). Another significant collaboration in the study of the structure of turbulence was the work done by the Soviet mathematical physicist KOLMOGOROV (1941) when turbulence was taken as a hierarchy of eddies of all different sizes where energy cascades from the largest to the smallest until being dissipated by the friction of molecules rubbing against one another. Besides those already quoted, many other physicists, mathematicians and engineers of 19^{th} and 20^{th} centuries have studied and collaborated for the understanding of the phenomenon. During late 1970's three main approaches for solving a turbulence problem computationally had been developed. These were the Reynolds Averaged Navier Stokes equations (RANS), Direct Numerical Simulation (DNS), and Large Eddy Simulation (LES). The latter is used and described in the present work and the other two are briefly addressed in order to enlighten the reader.

1.2 Literature Review

The LES model is a mathematical model for turbulence used in computational fluid dynamics, proposed initially by SMAGORINSKY (1963), to simulate atmospheric air currents. It is currently applied in a wide variety of engineering applications, including combustion and acoustics. A low pass filtering operation is the principal operation of the method. This filtering process works as an operator that filters out scales smaller than the mesh size POPE (2000). LEONARD (1997) defined a generalized filter as a convolution integral. The volume average box filter is the simplest filter used, implemented by DEARDORFF (1970), for which the resulting quantity is denoted as the resolvable scale filtered velocity.

For spectral methods the Fourier cutoff filter is used while for LES models the Gaussian filter is popular (see FERZIGER (1985)). There are other kinds of filters which are not even isotropic or homogeneous, but in all cases the filter introduces a scale that represents the smallest turbulence scale allowed by the filter.. The filter does an average process, it separates the resolvable scales from the sub grid scales. It is essentially used to derive the resolvable-scale equations. Except for the Fourier filter, that is build on sines and cosines, a second averaging produces a different result from the first averaging. This fact addresses LES dependence on the mesh and points out one of LES limitations. Different from the RANS, LES does not converge for the same result as we refine the mesh. Distinct turbulent structures can appear in different parts of the flow making it harder to predict the real turbulent flow. At the same time, it is well known that simple RANS models, such as the available $k-\epsilon$ model, do not reveal any secondary flow while LES is able to predict its motions magnitude. Even though some of these effects can be small, on the overall structure, they can represent an important effect on the flow.

LES operates on the Navier Stokes equations to reduce the range of length scales of the solution, thus reducing the computational cost. In the resolution of the conservation equation, the convective flux term is considered as a sum of tensors known as the Leonard stress, cross-term stress and the Subgrid Scale Reynolds stress (or SGS) (see LEONARD (1997)). The first removes a considerable part of the energy from the resolvable scales and is computed directly without the need of being modeled. However, sometimes this consideration can be inconvenient according to the numerical method used. For that, LEONARD (1997) proposed that, since the mean velocity is a smooth function, it could be represented in terms of its Taylor series expansion and be accurate; but only for low Reynolds number, as stated in CLARK (1977), through comparisons with DNS results. Another analysis, made by FERZIGER (1985), LEONARD (1997) and SHAANAN *et al.* (1975) state that the Leonard stresses, whenever a finite difference second order accuracy discretization is used, can be considered of the same order of the error truncation, thereby being implicitly represented. For the other two stress components, most validated cases model the sum of them and LES accuracy will depend on the chosen model for them as well. The fundamental problem of LES is to establish a satisfactory model for the SGS stresses. A significant portion of the turbulence spectrum is compounded by the subgrid scales and the impact of this unresolved shear layer on the overall flow structure must be modeled.

Different models for the SGS stresses have been proposed, varying from simple gradient diffusion models to more complex nonlinear stress strain rate. SMAGORINSKY (1963) was the first to propose a model for the SGS stresses

based on the assumption of homogeneous turbulence at the subgrid scales. The SGS stresses are taken to be proportional to the local rate of strain of the resolved flow. For this model, the SGS stresses follows a gradient diffusion process, similarly to molecular motion, and because of that, the Smagorinsky coefficient is calibrated for each flow and mostly kept constant throughout the flow. The success of the model is linked to its capacity to yield sufficient diffusion and dissipation to achieve stable numerical computations. The following model that has achieved significant improvement over the SMAGORINSKY (1963) model is known as Dynamic SGS Model, proposed by GERMANO *et al.* (1991). It is based on the SMAGORINSKY (1963) model approximation for the eddy viscosity but, instead of using a fixed value for the Smagorinsky coefficient, it is computed as LES proceeds, through the decomposition of the turbulent stresses using two filters. The first is based on the usual LES filter and the second, coarser, called the test filter, which examines the resolved fluctuations under lower wavenumber. The SGS stresses are modeled assuming the same Smagorinsky coefficient for the both filtering operations, where the test band should lie in the inertial subrange and the largest wavenumber should be kept far from the viscous region. Although dynamic models work really well, they reiterate in a more "aggressive way" the wrong assumption behind the mixing length formula, that eddies behave like molecules.

Regarding wall boundary conditions, the most common boundary encountered in confined fluid flow is the wall. The appropriate condition for the velocity components at solid walls is the no slip condition (u=v=0), in this case, wall functions can be used. The wall function models used in LES are the universal near wall model and the Werner Wengle model. For both methods y^+ (a dimensionless value) must be calculated for the first near wall node. Once it is calculated, the obtained value is compared with a range and classified according to it. If the obtained y^+ is less than 5, then the first node is in the viscous sublayer and nothing needs to be done. If the value obtained for y^+ is between 30 and 500, then the P node is in the fully turbulent region and the logarithm approximation should be used as a dampening solution for velocity. For the mixing length model, a mixing length is calculated, according to the type of flow, to compute the turbulent Reynolds stress adequately. Both $k-\epsilon$ and $k-\omega$ models require explicit wall damping functions to compute the Reynolds stress. For the present work, in order to avoid the iterative methods used for the LES method, the wall functions used follow the Werner Wengle model. This model counts with an analytical integration process for determining the velocity profile and then calculating the turbulent stress.

1.3 Objective

The objective of the present work is the implementation of a mathematical model for turbulence used in computational fluid dynamics (CFD) known as Large Eddy Simulation (LES) and the comparison of the values obtained for the variables of the model with the results obtained from the software *Fluent*, an extensively used software for CFD users. The implementation was performed in an existing bidimensional numerical model, based on the Finite Volume Method (FVM) for the simulation of natural system flows with high Reynolds Number (Re).

Once the implementation was made in a finite volume method program, the choice for the filter applied in LES was the cutoff length based on the grid scale. Once the model is bidimensional, the filter was proportional to the square root of the finite area dimensions. The Leonard stresses were considered of the order of the truncation error and, thus, were implicitly represented. The model used for the SGS stresses was the SMAGORINSKY (1963) model with the coefficient proposed by LILLY (1992). The wall function model used for the dampening of the velocity was the Werner Wengle model, with its analytical integration.

The set of differential equations governing the fluid flow problem was solved segregated where the coupling pressure-velocity is obtained by SIMPLEC algorithm. The variables are all co-located at the center of control volumes. To prevent the oscillations of the pressure-velocity coupling pressure field (checker-board) the interpolation Rhie-Chow family was used. In the process of discretization of the differential equations it is used the FVM process centered in the cell. The advective/convective terms of the conservation equations were discretized using techniques upwind/TVD with delayed correction (deferred correction). In the time it was used the Backward Euler Implicit method of second order (three levels). For the gradient reconstruction it was used the Green-Gauss method centered in the cell.

The sparse matrices generated in the process of discretization via FVM were stored in the CSR format (Compressed Sparse Row) for non symmetric matrices and CSRC (Compressed Sparse Row Column) for symmetric matrices. For the solution of symmetric linear systems it was used the conjugate gradient method with diagonal preconditioner (PCG), for the solution of non-symmetric linear systems it was used the biconjugate gradient stabilized method with diagonal preconditioner (BiCGSTAB).

Chapter 2

Conservation Laws of Fluid Motion

2.1 Governing Equations of the Fluid Flow

Although the analysis of turbulence is most seen in three dimensional fluid elements, the present work, as a matter of simplicity, without loss of generality, will describe all the governing equations in a two dimensional way. For numerous cases, the two dimensional analysis is a good approximation of the phenomenon.

For the mass conservation equation, the rate of increase of mass in a fluid element is equal to the net rate of flow of mass into the fluid element. The sum of the rate of change of density and the convective term in the mass conservation for a fluid element are represented as:

$$\frac{\partial \rho}{\partial t} + \frac{\partial (\rho u_j)}{\partial x_j} = 0. \tag{2.1}$$

From Newton's second law we know that the rate of increase of momentum of a fluid particle is equal to the sum of forces on the fluid particle. The components of the momentum equations are obtained by setting the rate of change of the fluid particle equal to the total force in the corresponding direction on the element due to surface stresses plus the rate of increase of momentum due to sources:

$$\frac{\partial (\rho u_i)}{\partial t} + \frac{\partial (\rho u_j u_i)}{\partial x_j} = -\frac{\partial P}{\partial x_j} + \frac{\partial \tau_{ij}}{\partial x_j} + \rho g_i. \tag{2.2}$$

In the above equations, ρ is the fluid density and u_i are the velocity components (i=1,2). Representing the sum of forces acting in the fluid we have: $\frac{\partial P_i}{\partial x_j}$ as the pressure gradient, $\frac{\partial \tau_{x_{ij}}}{\partial x_j}$ for the internal stresses on the fluid and ρg_i for the effect of buoyancy, caused by the gravitational field.

Conservation of energy of the fluid particle is ensured by equating the rate of change of energy of the fluid particle, to the sum of the net rate of work done on the fluid particle, the net rate of heat addition on the fluid and the rate of increase of energy due to sources:

$$\frac{\partial(\rho E)}{\partial t} + \frac{\partial(\rho u_j(E))}{\partial x_j} = \frac{\partial}{\partial x_j}\left(k\frac{\partial T}{\partial x_j}\right) - \frac{\partial(Pu_j)}{\partial x_j} + \frac{\partial}{\partial x_j}(\tau_{ji}u_i) + \rho g_i u_i + Q_H. \quad (2.3)$$

In equation (2.3), the parcel of potential energy has been incorporated through the term $\rho g_i u_i$. The total energy per unit mass is defined as the sum of internal i (thermal) and kinetic (mechanic) energy as follows:

$$E = i + \frac{1}{2}u_{ii}^2. \quad (2.4)$$

Fourier's law of heat conduction relates the local temperature gradient to the heat flux as follows:

$$\frac{\partial}{\partial x_j}\left(k\frac{\partial T}{\partial x_j}\right). \quad (2.5)$$

The term of power generation due to internal efforts is given by:

$$-\frac{\partial(Pu_j)}{\partial x_j} + \frac{\partial(\tau_{ji}u_i)}{\partial x_j}. \quad (2.6)$$

The energy flow can also be set through total enthalpy, H, and through sensitive enthalpy, respectively given by:

$$H = h + \frac{1}{2}u_{ii}^2, \quad (2.7)$$

where

$$h = i + \frac{P}{\rho}, \quad (2.8)$$

With equations (2.4), (2.8) and (2.9) it is possible to define energy E as:

$$E = H - \frac{P}{\rho}. \quad (2.9)$$

Substituting the expression (2.9) in equation (2.3) results in the conservation of energy, in the form of enthalpy:

$$\frac{\partial(\rho H)}{\partial t} + \frac{\partial(\rho u_j H)}{\partial x_j} = \frac{\partial}{\partial x_j}\left(k\frac{\partial T}{\partial x_j}\right) + \frac{\partial P}{\partial t} + \frac{\partial}{\partial x_j}(\tau_{ji}u_i) + \rho g_i u_i + Q_H. \tag{2.10}$$

The consideration of the hypothesis of thermodynamic equilibrium implies that the velocities of the thermodynamic processes are infinitely greater than the velocities of other processes. This leads to variations between thermodynamic quantities ρ, T, P and i to be practically instantaneous. Thus it is possible to define equations of state, usually given as:

$$P = P(\rho, T), \tag{2.11}$$

and

$$i = i(\rho, T). \tag{2.12}$$

For ideal gases, equations of state are given by:

$$P = \rho\left(\frac{R}{M_g}\right)T, \tag{2.13}$$

and

$$i = c_v T, \tag{2.14}$$

where $R = c_p - c_v$ is the ideal gases constant, c_p is the specific heat at constant pressure, c_v is the specific heat at constant volume, Mg is the molar mass of the gas, ρ is the gas density and T is the the gas temperature.

The behavior of the viscous stress defines the type of fluid modeled. For this class of fluids where the stresses are proportional to the rate of deformation, Newton's law of viscosity is used. This set of fluids is known as Newtonian fluids. Newton's law is given by:

$$\tau_{ij} = \mu\left(\frac{\partial u_i}{\partial x_j} + \frac{\partial u_j}{\partial x_i}\right) + \lambda\delta_{ij}\frac{\partial u_k}{\partial x_k}, \tag{2.15}$$

where μ is the dynamic viscosity and λ is the volumetric deformation of the fluid, also known, respectively, as the 2nd and 1st *Lame* parameters. For gases $\lambda = -\frac{2}{3}\mu$ is often used.

Substituting equation (2.15) in equation (2.2) results in:

$$\frac{\partial(\rho u_i)}{\partial t} + \frac{\partial(\rho u_j u_i)}{\partial x_j} = -\frac{\partial P}{\partial x_j} + \frac{\partial}{\partial x_j}\left(\mu\frac{\partial u_i}{)}\partial x_j\right) + \frac{\partial}{\partial x_j}\left(\mu\left(\frac{\partial u_j}{\partial x_i} + \lambda\delta_{ij}\frac{\partial u_k}{\partial x_k}\right)\right) + \rho g_i. \tag{2.16}$$

The above equations are known as the Navier Stokes equations (i=1,2).

The viscous dissipation term, $\frac{\partial}{\partial x_j}(\tau_{ji}u_i)$, in the total enthalpy equation (2.10) is also modified by the substitution of the stresses of equation (2.15), leading to:

$$\Phi = \mu\left[2\left[\left(\frac{\partial u_1}{\partial x_1}\right)^2 + \left(\frac{\partial u_2}{\partial x_2}\right)^2\right] + \left(\frac{\partial u_1}{\partial x_2} + \frac{\partial u_2}{\partial x_1}\right)^2 + \lambda\left(\delta_{ij}\frac{\partial u_k}{\partial x_k}\right)^2\right] > 0\,\forall i, j. \tag{2.17}$$

Specifically considering an ideal gas the final set of equation is given by:

$$\begin{cases} \frac{\partial \rho}{\partial t} + \frac{\partial}{\partial x_j}(\rho u_j) = 0 \\ \frac{\partial}{\partial t}(\rho u_i) + \frac{\partial}{\partial x_j}(\rho u_j u_i) = \frac{\partial}{\partial x_j}\left(\mu\frac{\partial u_i}{\partial x_j}\right) - \frac{\partial P}{\partial x_i} + \rho g_i + \frac{\partial}{\partial x_j}\left(\mu\left(\frac{\partial u_j}{\partial x_i} - \frac{2}{3}\delta_{ij}\frac{\partial u_k}{\partial x_k}\right)\right) \\ \frac{\partial}{\partial t}(\rho H) + \frac{\partial}{\partial x_j}(\rho u_j H) = \frac{\partial}{\partial x_j}\left(k\frac{\partial T}{\partial x_j}\right) + \frac{\partial P}{\partial t} + \Phi + \rho g_i u_i + Q_H \\ P = \rho\left(\frac{R}{M_g}\right)T \\ H = c_p T + \frac{1}{2}u_{ii}^2. \end{cases} \tag{2.18}$$

The above mathematical model has six equations: one for mass conservation, two for momentum (i=1,2), one energy equation for total enthalpy and two equations of state. The variables are density, ρ, the components u_1 and u_2 of the velocity vector, pressure, P, total enthalpy, H, and temperature, T. Dynamic viscosity μ, the diffusion coefficient, k, and the specific heat, c_p, are smooth functions known through temperature, T. The above set of equations can be simplified for low Mach numbers [1], below 0.3.

[1] is a dimensionless quantity representing the ratio of flow velocity past a boundary to the local speed of sound: $M = \frac{u}{c}$

2.2 Slightly Compressible Flow

2.2.1 Natural and Forced Convection

Although numerous forcing terms can induce the flow of a fluid, it is common to fit them into two categories: forced and natural convection. The flows caused by a pressure gradient or superficial forces are usually classified as flow by forced convection. Flows caused by mass force field are known as flows by natural convection, the most common natural flow is due to gravitational field.

Natural flows are caused by variation of the fluid specific mass, one of the approximations for this kind of flow with low velocity is the Boussinesq model, but this approximation is only valid for small variations of specific mass and temperature. This model is very useful for fluid flows like water. For gases with high temperature gradients this approximation can produce errors. For the present work the flow of the gas has low velocity and high temperature gradients.

The equation set (2.18) is simplified for low Mach number in order to remove all the compressible effects of the specific mass variation caused by the pressure field, however, allowing the compressible effects on the specific mass caused by high temperature variations. This simplified set of equation is known as slightly compressible or simply flow with low Mach number.

The first step in the simplification of the model is to filter the effects of the pressure acoustic waves in the environment. From the non dimensional analysis when the Mach number tends to zero, it is shown that it is enough to decompose pressure into two parcels: thermodynamic (or background) and hydrodynamic (incompressible). It is done to filter the acoustic effects of pressure. Thermodynamic parcel is homogenous in space while the hydrodynamic parcel keeps its variation in both time and space. In natural convection problems, it is usual to make hydrostatic pressure explicit, in order to avoid numerical errors caused by the difference of order of magnitude between hydrostatic and hydrodynamic pressures. The filtering process is represent as:

$$P(x_i, t) = P_0(t) + \rho_{ref}\, g_i\, x_i + \tilde{P}(x_i, t), \tag{2.19}$$

where ρ_{ref} is the specific reference density of the undisturbed fluid.

If we substitute equation above into the momentum equations (2.16) we have:

$$\frac{\partial(\rho u_i)}{\partial t}+\frac{\partial(\rho u_j u_i)}{\partial x_j} = \underbrace{-\frac{\partial \tilde{P}_i}{\partial x_j}}_{\text{IV}} + \underbrace{(\rho-\rho_{ref})g_i}_{\text{V}} + \frac{\partial}{\partial x_j}\left(\mu\frac{\partial u_i}{\partial x_j}\right)+\frac{\partial}{\partial x_j}\left(\mu\left(\frac{\partial u_j}{\partial x_i}-\frac{2}{3}\delta_{ij}\frac{\partial u_k}{\partial x_k}\right)\right). \tag{2.20}$$

In the above equation the thermodynamic pressure disappears and hydrostatic pressure is incorporated in term (V). The hydrodynamic pressure is the only pressure parcel that remains in its initial form. Regarding forcings, forced convection is caused by term (IV), and natural convection is caused by term (V).

Still, for the simplification for low Mach number, the total enthalpy definition can be simplified as:

$$H = h, \tag{2.21}$$

for the simplification above, the kinematic energy parcel is neglected. For ideal gases, with multiple components, it is useful to redefine total enthalpy as:

$$H = \int_{T_{ref}}^{T} c_p dT, \tag{2.22}$$

where T_{ref} is the reference temperature.

For the energy equation, the heat flux can be approximated by the total enthalpy flux through equation (2.10), therefore:

$$k\frac{\partial T}{\partial x_j} \approx \frac{k}{c_p}\frac{\partial H}{\partial x_j}. \tag{2.23}$$

The derivative pressure term of the energy equation stays only as a thermodynamic pressure function given by:

$$\frac{\partial P}{\partial t} \approx \frac{\partial P_0}{\partial t}. \tag{2.24}$$

It can, by simplicity, be neglected, similarly to what happens to the dissipation term, Φ, and with and the potential energy term, $\rho g_i u_i$. After all those considerations, the total enthalpy energy equation for low Mach number is given by:

$$\frac{\partial}{\partial t}(\rho H) + \frac{\partial}{\partial x_j}(\rho u_j H) = \frac{\partial}{\partial x_j}\left(\frac{k}{c_p}\frac{\partial H}{\partial x_j}\right) + Q_H. \tag{2.25}$$

The state equation also changes to consider only the thermodynamic pressure, decoupling the state equation of hydrodynamic pressure. The new equation of state results in:

$$\rho = \frac{P_0(t) M_g}{RT}. \tag{2.26}$$

The set of equations for the flow of an ideal gas in forced and natural convection regime for low velocities is given by:

$$\begin{cases} \frac{\partial \rho}{\partial t} + \frac{\partial (\rho u_j)}{\partial x_j} = 0 \\ \frac{\partial (\rho u_i)}{\partial t} + \frac{\partial (\rho u_j u_i)}{\partial x_j} = -\frac{\partial P}{\partial x_j} + (\rho - \rho_{ref}) g_i + \frac{\partial}{\partial x_j}\left(\mu \frac{\partial u_i}{\partial x_j}\right) + \frac{\partial}{\partial x_j}\left(\mu \left(\frac{\partial u_j}{\partial x_i} - \frac{2}{3}\delta_{ij}\frac{\partial u_k}{\partial x_k}\right)\right) \\ \frac{\partial}{\partial t}(\rho H) + \frac{\partial}{\partial x_j}(\rho u_j H) = \frac{\partial}{\partial x_j}\left(\frac{k}{c_p}\frac{\partial H}{\partial x_j}\right) + Q_H \\ \rho = \frac{P_0(t) M_g}{RT} \\ H = \int_{T_ref}^{T} c_p dT. \end{cases} \tag{2.27}$$

The above mathematical model has six equations: one for the mass conservation, two momentum equations (i=1,2), one energy equation for total enthalpy and two equations of state. The variables are: the specific mass ρ, the velocity components u_1 and u_2, hydrodynamic pressure $\tilde{P}$, total enthalpy H and temperature T. The dynamic viscosity μ, the diffusion coefficient k and the specific heat c_p can be smooth functions known through temperature T.

For the solution of the set of equations 2.27 a method that handles coupling between the conservation equations is needed. A simple approach would be to solve the system of equation simultaneously, i.e., set up a system of equations involving all the variables to solve this system of simultaneous equations. The nonlinearities in this approach are treated iteratively by methods such as the Newton-Raphson method. Another possibility is the resolution of segregated equation systems, i.e., each variable has its own systems of equations. In this approach, both nonlinearities and the coupling of the variables are treated in the same iterative process. The family of SIMPLE algorithm derives from this segregated approach solution. For this work, the version of SIMPLE (Semi-Implicit Method for Pressure Linked Equations) entitled SIMPLEC (SIMPLE-Consistent) was used as described in details in CARVALHO (2014).

The SIMPLEC solution algorithm follows the sequence for each time step:

1. Estimate of fields $P^* = P^n$, $\vec{v} = \vec{v}^n$ and $\rho = \rho^n$ of time n;
2. Assemble discretized momentum equations;
3. Solve the momentum discretized equations and get $\vec{v}^{\vec{*}}$;
4. Assemble and solve the correction of pressure equation and get P';
5. Update the velocities and pressure values;
6. Assemble and solve the equation of energy using the updated field $\vec{v}$ and get H;
7. Get the temperature using the equation of state;
8. Get the new density field through the equation of state;
9. Check the convergence of the method. If all the convergence criteria are not satisfied return to (2) and continue the iterative process.

Chapter 3

Turbulence

Turbulence is the state of fluid motion which is characterized by apparently random and chaotic three-dimensional vorticity. Turbulence usually results in increased energy dissipation, mixing, heat transfer and drag. Turbulence is not really chaos since turbulent flows are not only time-dependent, but space dependent as well.

Most turbulence researchers believe that the solutions of the fluid mechanical equations are deterministic. Just like the solutions of non-linear dynamical systems, it is believed that turbulent solutions are determined by their boundary and initial conditions. And like non-linear dynamical systems, these deterministic solutions of the non-linear fluid mechanics equations exhibit a behavior that appears for all intents and purposes to be random. Such solutions are called turbulent, and the phenomenon turbulence. Because of this chaotic-like and apparently random behavior of turbulence, statistical techniques are needed for most of turbulence studies.

Nowadays turbulence remains an unsatisfactory topic since scientists have not completely understood the phenomenon. It remains as a fundamental challenge to scientists and engineers, since most technologically important flows are turbulent.The advances in understanding over the past few decades, together with the advent of large scale computational and experimental capabilities, present the scientist and engineer with the first real capabilities for understanding and managing turbulent flows.

In 1937, Taylor and von Karman proposed the following definition of turbulence as cited in VERSTEEG and MALALASEKERA (2007):

"Turbulence is an irregular motion which in general makes its appearance in fluids, gaseous or liquid, when they flow past solid surfaces or even when neighboring streams of the same fluid flow past or over one another"

Turbulent flow occurs at high Reynolds numbers and is dominated by inertial forces, which tend to produce chaotic eddies, vorticity and other flow instabilities. The Reynolds number is defined as the ratio of inertial forces to viscous forces, consequently defining the importance of these two types of forces for given flow conditions. It is defined as follows:

$$R_e = \frac{\rho\, v\, L}{\mu}, \tag{3.1}$$

where:

ρ is the density of the fluid (kg/m^3);

v is the mean velocity of the object relative to the fluid $(SIunits : m/s)$;

L is a characteristic linear dimension (m);

μ is the dynamic viscosity of the fluid $(Pas = Ns/m^2 = kg/(ms))$.

3.1 Turbulence and its Effects on the Mean Flow

The appearance of turbulent fluctuations results in the momentum exchange due to convective transport by the eddies, so the faster moving fluids start to move slowly and the slower ones to move faster. As a consequence of this process, the fluid layers start to experience additional turbulent shear stresses, the Reynolds stresses. Also, temperature or concentration gradients will result in eddies generating turbulent heat or concentration fluxes across the control volume boundaries.

I will use an approach by which turbulence is treated and studied from a statistical point of view. It starts by applying the decomposition of the flow into its mean and fluctuating components. By applying this decomposition to the transport equations of momentum and kinematic energy, it is possible to isolate some of the mechanisms by which the turbulence affects the mean flow.

3.1.1 Reynolds Averaged Equations

The Reynolds Averaged Navier Stokes equations (or RANS equations) are time-averaged equations of motion for fluid flow. They are obtained through a time average process of the governing equations. Together with the continuity equation it governs every turbulent flow. The idea behind the RANS equations is the Reynolds

decomposition, where the flow variables are decomposed into a mean value (time averaged) and a fluctuating component:

$$u_i = \overline{u}_i + u_i'. \tag{3.2}$$

where the $\overline{u}_i$ is the mean velocity and u_i' is the fluctuation with respect to the mean value.

RANS are used for flows where the variation of the density can be neglected. The reasons for the previous statement are the additional terms that arise when Reynolds average is used. It is possible to analyze it through the continuity equation. First, the Reynolds average continuity equation for a constant density flow is described. Later, the Reynolds average continuity equation for a flow where the density variations can not be neglected is described for the comparison.

$$\frac{\partial \rho}{\partial t} + \frac{\partial(\rho \overline{u_i})}{\partial x_j} = 0, \tag{3.3}$$

The time averages for individual terms of the continuity equation considering density fluctuations according to the Reynolds decomposition can be written as follows:

$$\overline{\frac{\partial \rho}{\partial t}} = \frac{\partial \overline{\rho}}{\partial t}, \tag{3.4}$$

$$\overline{\rho u_i} = \overline{\rho}\,\overline{u}_i + \overline{\rho' u_i'}. \tag{3.5}$$

As a result, the continuity equation is written as follows:

$$\frac{\partial \overline{\rho}}{\partial t} + \partial \frac{(\overline{\rho}\,\overline{u}_i)}{\partial x_j} + \partial \frac{\overline{(\rho' u_i')}}{\partial x_j} = 0. \tag{3.6}$$

Comparing equations 3.3 and 3.6, it is easy to see the additional terms that arise from the correlation of the density and velocity fluctuations, and need to be modeled.

An artifice to reduce the number of separate terms that need to be modeled, is to use a density weighted averaging procedure, called Favre averaging. According to the Favre's approach for any dependent variable, a density weighted mean property can be described as YEOH and YEUN (2009):

$$\tilde{\phi} = \frac{\overline{\rho\phi}}{\overline{\rho}}. \tag{3.7}$$

The instantaneous variable is written as follows:

$$\phi = \tilde{\phi} + \phi''. \tag{3.8}$$

where:

$\tilde{\phi}$ is the mean value;
ϕ'' is the fluctuation of ϕ with relation to its mean value also including the density fluctuation effects.

The time averages for individual terms of the continuity equation considering density fluctuations according to the Favre's decomposition can be written as follows:

$$\overline{\frac{\partial u_i}{\partial t}} = \frac{\partial \overline{u}_i}{\partial t}, \tag{3.9}$$

$$\overline{\rho u_i} = \overline{\rho}\tilde{u}_i + \overline{\rho u_i''}. \tag{3.10}$$

where: $\overline{\rho u_i''} = 0$ (according to the construction of Favre's averaging process.)

As a result, the continuity equation is written as follows:

$$\frac{\partial \overline{\rho}}{\partial t} + \partial \frac{(\overline{\rho}\tilde{u}_i)}{\partial x_j} = 0. \tag{3.11}$$

Comparing equations 3.6 and 3.11 it is easy to see the reduction of additional terms by using the Favre averaging process.

Note that, if the flow is incompressible (the density is constant), then, $\tilde{u}_i = \overline{u}_i$ and $u_i'' = u_i'$, i.e., Favre's decomposition to flows with constant density is reduced to the Reynolds decomposition.

By an analogous procedure it is possible to obtain the time average momentum equations:

$$\frac{\partial \overline{\rho}\,\tilde{u}_i}{\partial t} + \frac{\partial(\overline{\rho}\tilde{u}_j\tilde{u}_i)}{\partial x_j} = -\frac{\partial \overline{P}}{\partial x_j} + \frac{\partial(\mu\, grad\, \tilde{u}_i)}{\partial x_j} - \frac{\partial \overline{(\rho u_j'' u_i'')}}{\partial x_j} + S_{Mi}. \tag{3.12}$$

Where $\overline{\rho u_j'' u_i''}$ needs to be modeled. (S_{Mi} includes the linear source terms).

By an analogous procedure it is possible to obtain the time average equations for an scalar property:

$$\frac{\partial(\overline{\rho}\,\tilde{\phi})}{\partial t} + \partial\frac{(\overline{\rho}\,\tilde{u}_i\,\tilde{\phi})}{\partial x_j} = \frac{\partial}{\partial x_j}\left[\Gamma_\phi grad\tilde{\phi}\right] - \frac{\partial\overline{(\rho u_j'' \phi'')}}{\partial x_j} + S_\phi, \tag{3.13}$$

Where $\overline{\rho u_j'' \phi''}$ needs to be modeled.

where Γ_ϕ is the diffusion coefficient that can be defined as $\Gamma = \mu/Pr$, and Pr represents the Prandtl number, a dimensionless number that defines the ratio of momentum diffusivity (dynamic viscosity) to thermal diffusivity as follows:

$$Pr = \frac{\mu C_p}{k}, \tag{3.14}$$

3.1.2 Turbulence Models

To be able to compute turbulent flows with RANS equations, turbulence models have to be developed to predict the Reynolds stresses and the scalar transport terms in order to close the system of the mean flow equations. Useful models must be simple, accurate, economical and have a wide applicability. Turbulent models are classified based on the number of extra transport equations needed to solve with the RANS equations.

The mixing length, k-ϵ and k-ω are the most widely used and validated models, based on the presumption that there exists an analogy between the action of viscous stresses and Reynolds stresses on the mean flow. These models will be briefly addressed in order to enable the reader to evaluate the development of turbulence models.

3.1.3 Mixing Length Model

BOUSSINESQ (1871), PRANDTL (1963) introduced the additional concept of the mixing length: Prandtl mixing length model (PMLM). A method attempting to describe momentum transfer by turbulence Reynolds stresses with a Newtonian fluid boundary layer by means of an eddy viscosity. It assumes that turbulent motions can be characterized by the length scale of the eddies. The effective viscosity is taken as being proportional to the square of a quantity having the dimensions of length multiplied by the absolute value of the local velocity gradient.

The calculations of the method are easy to make and cheap in terms of computing resources because no additional differential equation must be solved. In unbounded flows, the variation of the Prandtl mixing length across the layer width is not large, so that velocity profiles can be fairly well predicted. Although the method does not give good predictions close to a wall it can be modified through the use of near wall damping functions to handle the processes occurring there adequately. It is such a well established method that for most boundary layer flows, at least the order of magnitude of the mixing length can be correctly guessed. On the other hand, PMLM is completely incapable of describing flows with separation and recirculation. The method implies that the local level of turbulence depends only upon the local generation and dissipation rates; while truly turbulence may be carried or diffused to locations where no turbulence is actually being generated at all. Another disadvantage of PMLM is that it implies that the turbulent viscosity is always positive when in reality it can change sign.

3.1.4 The $k - \epsilon$ Model

Is a two equation model to represent the turbulent properties of the flow with two extra transport equations . The first transported variable is turbulent kinetic energy, k. The second transported variable in this case is the turbulent dissipation, ϵ. The latter is the variable that determines the scale of the turbulence, whereas the first variable, k, determines the energy in the turbulence.

The $k - \epsilon$ model was originally developed to improve the mixing length model and avoid the algebraic prescription of the turbulent length scale in complex flows. This model has given good results for free shear layer flows with relatively small pressure gradients and requires explicit wall damping functions and the use of fine grid spacing near solid walls. For wall bounded flows, it agrees with experimental results for zero and small mean pressure gradients, meanwhile being less accurate for large adverse pressure gradients.

3.1.5 The $k - \omega$ Model

Like the $k - \epsilon$, the $k - \omega$ is also a well known and widely tested two equation eddy viscosity model. It is an alternative to define the eddy viscosity function and the convective transport equations are solved for the turbulent kinetic energy and its specific dissipation rate, k and ω, respectively.

According to BARDINA *et al.* (1997), this model is superior in numerical stability to the $k - \epsilon$ specially in the viscous sublayer near the wall. It does not

require explicit wall damping functions as the other two equation models because of the large values of ω in the wall region. The numerical wall boundary conditions require the specification of the distance from the wall to the first point of the wall. In the logarithmic region, the model gives good agreement with experimental results for adverse pressure gradient flows.

3.2 Advanced Models

Different complexities show up and great efforts are made to develop RANS turbulence models but the need of a more general model with a wider applicability is noteworthy. The point that calls attention to the development of more comprehensive models is exactly the distinct behavior of large and small eddies. Some of those advanced models will be addressed in this topic to discuss about this distinction.

3.2.1 Direct Numerical Simulation

The Direct Numerical Simulation (or DNS) is a simulation where the whole range of spatial and temporal scales of turbulence have to be resolved in the computational mesh, respecting the Kolmogorov scales, from the smallest dissipative scales up to the integral scale of the largest eddies, associated with motions containing most of the kinetic energy. The Kolmogorov scale is given by a relation between the kinematic viscosity, μ, and the rate of dissipation, ϵ. For this method, the unsteady Navier Stokes equations are solved on spatial grids which are sufficiently discretized to solve the Kolmogorov length scales at which energy dissipation takes place and with small enough time step to resolve the period of fastest fluctuations. The memory storage of this method grows fast with the Reynolds number and the calculation is very expensive when thinking about computing resources which makes it unfeasible for industrial purposes.

A method which is in middle route between DNS and RANS, it is called Large Eddy Simulation (LES) and is more accurate and requires more computing time than RANS but at the same time can work on larger Reynolds number and more complex flows (check figure 3.1). DNS and LES require to solve the instantaneous Navier Stokes equations in time and three dimensional space but LES could be described as a simulation for large scales and RANS for small scales.

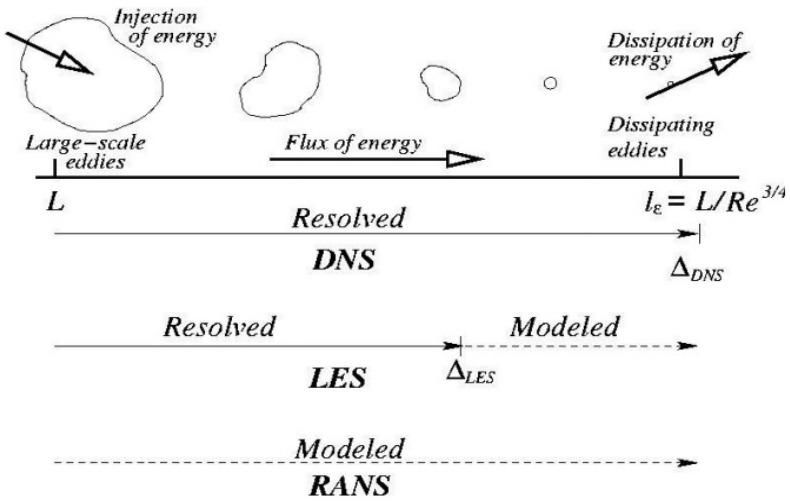

Figure 3.1: Turbulence Scales and Prediction Models

3.2.2 Large Eddy Simulation

Since large and small eddies show differences in behavior, a suitable and widely applicable model for the representation is needed. The larger eddies interact with the mean flow extracting energy from it and are more anisotropic while their behavior is dictated by the geometry of the problem domain as well as boundary conditions and body forces. The smaller eddies are nearly isotropic and have a more universal behavior, when the turbulent flow has high enough Reynolds number. This differences in behavior of large and small eddies inspired a different approach to the computation of turbulent flows. The essence of the large eddy simulation approach to the numerical treatment of turbulence is that large eddies (affected by the boundary conditions and carrying most of the Reynolds stresses) must be computed while the small scale turbulence which is weaker and contributes less to the Reynolds stress being therefore less critical, are more amenable to modeling.

In 1941, Kolmogorov introduced the idea that turbulent motions span a wide range of scales ranging from a macro scale at which the energy is supplied, to a micro scale at which energy is dissipated by viscosity. The interaction among the eddies of various scales passes energy sequentially from the larger eddies gradually to the smaller ones. This process is known as the turbulent energy cascade.

This process starts with the eddies, that are a swirling of fluid mass created when the fluid flows past an obstacle. There are eddies of different sizes in a turbulent flow. If we consider a channel we can have a large eddy (the largest eddy) which is of the system length (its diameter is of the same order of the channels width) and we can

have small eddies that are of molecular length scale. The process takes place with the large eddies extracting the energy from the mean flow because of its instabilities that trigger turbulence. Due to these instabilities, once large eddies extract energy from the mean flow, they will evolve into smaller and smaller eddies through which energy subsequently pass. Consequently, energy will pass from the large eddies to the smaller eddies in this way until it reaches the smallest eddy. Thus, the entire energy cascades through smaller and smaller eddies, until it is mopped up by the smallest eddy due to viscous dissipation. Energy can not be mopped up into viscous dissipation by the large eddies because the length scale of them is of the order of the system length scale. Therefore, if the Reynolds number is large relatively to the system length scale, the inertia forces dominate over viscous force. The process described is illustrated in figure 3.2:

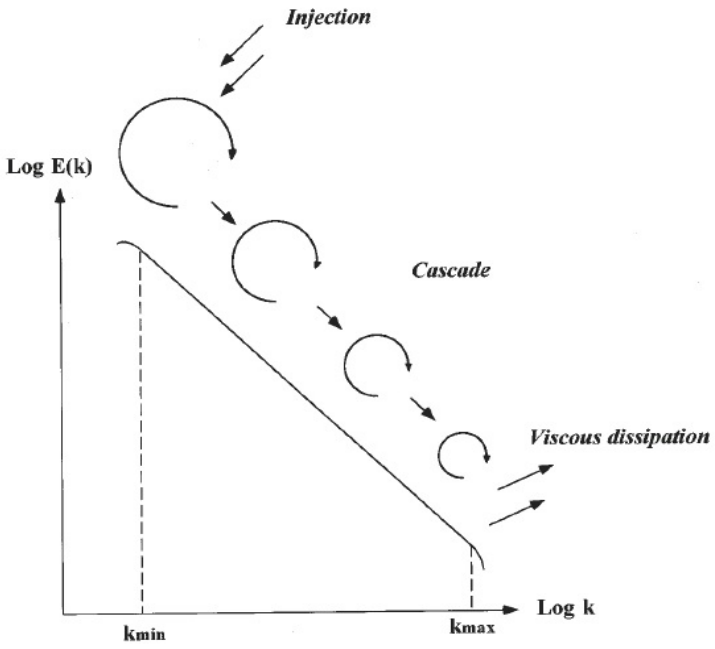

Figure 3.2: Depiction of Energy Cascade.

In the above figure, E represents the turbulence spectra and k represents the corresponding wavenumber.

In figure (3.2) in the horizontal axis, k represents the wavenumbers (energy moves to smaller wavenumbers characterizing the turbulent cascade process), while in the vertical axis, E represents the energy spectrum.

It can be said that the eddies know how big they are, at which rate energy is supplied to them and at which rate they must supply it to the next smaller eddies in the cascade. The implication is that the smallest eddies have the lowest speeds,

while the largest ones have the highest speeds and thus contain the bulk of the kinetic energy.

3.2.3 Filtering

Since LES counts with the computation of large eddies in the grid, a spatial filtering operation is defined by means of a filter function, G, as follows:

$$\bar{\phi}(x,t) = \int\int\int G(x-\xi;\Delta)\phi(\xi,t)d^3\xi, \tag{3.15}$$

where:

G = a filter function;

$\bar{\phi}(x,t)$ = filtered function;

$\phi(x,t)$ = original (unfiltered) function;

Δ = filter cutoff width.

Equation (3.15) shows that filtering is an integration, just like time averaging in the development of the RANS equations. In LES the integration is not over time but rather a spatial filtering (2D in the present work).

The method starts with the selection of a filtering function and the selection of a cutoff width Δ given by:

$$\Delta = (\Delta_x\Delta_y\Delta_z)^{\frac{1}{3}}, \tag{3.16}$$

for a 3D model. Both the filtering function and the cutoff width are chosen to resolve all those eddies with a length scale greater than the cutoff width for a unsteady flow computation.

During spatial filtering, information relating to the smaller turbulent eddies is lost. Interaction effects between the larger, resolved eddies and the smaller unresolved ones, gives rise to sub-grid-scale stresses or SGS stresses and its effect on the resolved flow must be described by a SGS model of the unresolved stresses.

If finite volume is the method used, the time dependent, space-filtered flow equations are solved on a grid of control volumes (mean flow and all turbulent eddies at scales larger than (3.15)) along with the SGS model of the unresolved stresses.

3.2.4 Filtered Equations

It is possible to use the same filtering function $G(x, x') = G(x - x')$ throughout the computational domain, i.e., G is independent of position x, using considerable algebraic simplification. Given that the filtering operation is linear it is possible to swap the order of the filtering and differentiation with respect to time, as well as the order of filtering differentiation with respect to space coordinates.

In most LES of compressible flows, the flow variables are Favre averaged or density weighted, thus, for the standard LES filtering technique, we find the following equation for mass conservation:

$$\frac{\partial \overline{\rho}}{\partial t} + \frac{\partial (\overline{\rho} \tilde{u}_i)}{\partial x_j} = 0, \tag{3.17}$$

where tilde indicates a filtered flow variable.

Applying the filter to the momentum equation we get the LES momentum equation:

$$\frac{\partial \overline{\rho} \tilde{u}_i}{\partial t} + \frac{\partial (\overline{\rho}\, \tilde{u_j}\, \tilde{u_i})}{\partial x_j} = -\frac{\partial \overline{\sigma_{ij}}}{\partial x_j} - \frac{\partial}{\partial x_j} \underbrace{\overline{\rho}(\overline{u_j u_i} - \tilde{u}_j \tilde{u}_i)}_{\text{VI}} + S_{Mi}. \tag{3.18}$$

Term VI is commonly termed as the sub grid scale stresses and a substantial portion of τ_{ij} is attributable to convective momentum transport due to interactions between the unresolved or SGS eddies.

$$\overline{\sigma}_{ij} = \overline{P}\delta_{ij} - \mu \left(\frac{\partial \tilde{u_j}}{\partial x_i} + \frac{\partial \tilde{u_i}}{\partial x_j} \right) + \frac{2}{3}\mu \frac{\partial \tilde{u_j}}{\partial x_i} \tag{3.19}$$

3.2.5 The Smagorinsky Model

According to POPE (2000), SMAGORINSKY (1963) was the first to postulate a model for the SGS stresses. Intimate connection between turbulence production and mean strain, according to the Boussinesq eddy viscosity hypothesis, was found to give good predictions of Reynolds averaged turbulent stresses. Turbulent stresses are found to increase as the mean rate of deformation increases, i.e, turbulent stresses are proportional to the mean rate of strain. The τ_{sgs} stress is modeled as a single entity by means of a single SGS turbulence model as follows:

$$(\overline{\rho u_j u_i} - \overline{\rho}\tilde{u_j}\tilde{u_i}) = \tau_{sgs} - \frac{1}{3}\tau_{ii}\delta_{ij} = -2\mu_{sgs}\bar{S_{ij}} = -\mu_{sgs}\left[\frac{\partial \bar{u_i}}{\partial x_j} + \frac{\partial \bar{u_j}}{\partial x_i}\right] + \frac{1}{3}\tau_{ii}\delta_{ij}. \quad (3.20)$$

The model is based on isotropic eddy viscosity where $\bar{S_{ij}} = \frac{1}{2}(\partial \bar{u}_i/\partial x_j + \partial \bar{u}_j/\partial x_i)$ is the resolved rate of strain tensor and δ_{ij} is the Kronecker delta defined as:

$$\delta_{ij} = \begin{cases} 0 \;\; if \;\; i \neq j \\ 1 \;\; if \;\; i = j. \end{cases} \quad (3.21)$$

The model is built on PMLM (3.3.3) assuming that the kinematic viscosity ν_{sgs} can be described as:

$$\nu_{sgs} = v \;\; l, \quad (3.22)$$

where v and l are the velocity and length scale, respectively, and is related to the dynamic viscosity by:

$$\nu_{sgs} = \frac{\mu_{sgs}}{\rho}. \quad (3.23)$$

Taking the length scale as the filter width Δ (3.16), the velocity v can be represented as the product of length scale and the average strain rate of the resolved flow. Thus, the **SGS viscosity** is evaluated as follows:

$$\mu_{sgs} = \rho(C_{sgs}\Delta)^2|\bar{S}| = \rho(C_{sgs}\Delta)^2\sqrt{2\bar{S}_{ij}\bar{S}_{ij}}. \quad (3.24)$$

Different values of C_{sgs} are due to the effect between the mean flow, shear and strain, somehow showing that the behavior of small eddies are not as universal as it was thought and suggesting a case by case analysis and choice of the C_{sgs} value. The range varies between $C_{sgs} = 0.1$ to $C_{sgs} = 0.24$. In the present work the assumed value for the constant was taken according to DEARDORFF (1970) that suggested that for LES computations of turbulent channel flow, with strongly anisotropic turbulence, particularly in near wall regions C_{sgs} should be taken as 0.1, so excessive damping was not going to happen and that this value would be appropriate for internal flow calculations.

The final set of equations for the model for a compressible flow is as follows:

$$\begin{cases} \frac{\partial(\overline{\rho})}{\partial t} + \frac{\partial}{\partial x_j}(\overline{\rho}\,\tilde{u}_j) = 0 \\ \frac{\partial}{\partial t}(\overline{\rho}\tilde{u}_i) + \frac{\partial}{\partial \tilde{u}_j}(\overline{\rho}\tilde{u}_j\tilde{u}_i) = \frac{\partial}{\partial x_j}\left((\mu+\mu_{sgs})\frac{\partial \tilde{u_i}}{\partial x_j}\right) - \frac{\partial \overline{P}}{\partial x_i} + (\overline{\rho}-\overline{\rho}_{ref})g_i + \\ \frac{\partial}{\partial x_j}\left((\mu+\mu_{sgs})\left(\frac{\partial \tilde{u_j}}{\partial x_j} - \frac{2}{3}\delta_{ij}\frac{\partial \tilde{u_k}}{\partial x_k}\right)\right) \\ \frac{\partial}{\partial t}(\rho\tilde{H}) + \frac{\partial}{\partial x_j}(\rho u_j\tilde{H}) = \frac{\partial}{\partial x_j}\left(\frac{\mu}{Pr} + \frac{\mu_{sgs}}{Pr_{sgs}}\right) + Q_H. \end{cases} \tag{3.25}$$

The above model for the present work counts with four equations: mass conservation, two momentum equations and one transport equation for enthalpy.

3.2.6 Wall Functions

Near the wall, μ_{sgs} increase considerably, becoming quite large because velocity gradients are high at that point. At the interface between the fluid and the surface, there exists an attraction between the molecules or atoms that make up the fluid and those that make up the solid. This attractive force is strong enough to reduce the bulk velocity of the fluid to zero. So the bulk velocity of the fluid must change from whatever its value is far away from the wall to a value of zero at the wall, called the no slip condition. The most powerful consequence of the no slip condition is the appearance of strong velocity gradients near the wall. This region is often very thin, and it is then called a boundary layer. Within the boundary layer, adjacent layers of fluid are in relative motion, and because all fluids have viscosity, there will be friction between the layers as they slide over each other. In other words, viscous stresses are produced, with a magnitude given by the viscosity times the velocity gradient as follows:

$$\tau_{sgs} = \nu_{sgs}\bar{S}_{ij}. \tag{3.26}$$

These viscous, frictional stresses cause energy dissipation in the fluid, which appears as heat. Since the SGS turbulent fluctuations near the wall go to zero, in the same manner, ν_{sgs} must go to zero. The standard Smagorinsky model eddy viscosity is nonzero at solid boundaries, which is contrary to the notion that the eddy viscosity should be zero where there is no turbulence. The easy fix for this situation is to add a VAN DRIEST (2012) style damping function into the length scale that can be described as:

$$f_u = 1 - exp(-y^+/25). \tag{3.27}$$

And then multiply μ_{sgs} by (3.20) as follows:

$$\mu_{sgs} = \rho(f_u C_s \Delta)^2 \bar{S}_{ij}. \tag{3.28}$$

y^+ is a non dimensional wall distance for a wall-bounded flow and to accurately represent the structures near wall region. To represent accurately the structures in the near-wall region, the first grid point must be located at $y^+ \leq 1$, thus

$$y^+ = \frac{u_{fr}\ y}{\nu}, \tag{3.29}$$

where u_{fr} is the friction velocity at the nearest wall, y is the distance to the nearest wall and ν is the local kinematic viscosity of the fluid.

For the present work, it will be used the implementation of the near wall model used was WERNER and WENGLE (1993)'s model, to avoid the iterative solution procedure required for determining the friction velocity u_{fr}. They proposed an analytical integration of power law near wall velocity distribution, resulting in the following expressions for the wall shear stresses τ_w:

$$\tau_w = \begin{cases} \frac{2\mu|u_p|}{\Delta} \quad for \ \ |u_p| \leq \frac{\mu}{2\rho\Delta} A^{2/(1-B)} \\ \rho \left[\frac{1-B}{2} A^{\frac{1+B}{1-B}} (\frac{\mu}{\rho\Delta})^{1+B} + \frac{1+B}{A} (\frac{\mu}{\rho\Delta})^{B} \ |u_p| \right]^{\frac{2}{1+B}} \quad for \ \ |u_p| \geq \frac{\mu}{2\rho\Delta} A^{2/(1-B)}, \end{cases} \tag{3.30}$$

where $|u_p|$ is the velocity parallel o the wall, A=8.3, B=1/7, Δ=near wall control volume lentgh scale.

Once we calculate τ_w it is possible to calculate u_{fr} which is described as:

$$u_{fr} = \left(\frac{\tau_w}{\rho} \right)^{1/2}. \tag{3.31}$$

Having quantities (3.23) and (3.24) we calculate (3.22) followed by the calculation of (3.20) and then substitute the value of f_u in (3.21) to finally obtain the adequate value of μ_{sgs} that respects the decay rate of energy.

Chapter 4

Results

4.1 General Criteria and Parameters

The problem chosen was a square closed cavity of 1 by 1 square meters. To compare the results obtained in the implemented model, the software *Fluent* 15, developed by the engineering simulation software Ansys, was used. In *Fluent*, simulations were performed with the following settings: double precision in calculations and SIMPLEC method, as was explained in chapter 3. The square cavity problem considers a square compartment closed in the four edges. In all sides the tangential and normal speeds are zero, corresponding to the non-slip condition for a impermeable wall. The air inside starts with a standby temperature of $10°C$. The left vertical wall has a temperature, T_h, higher than the air temperature inside, while the right wall has a lower temperature, T_c, when compared to the air temperature. The horizontal walls are insulated. The illustrative scheme of the problem is as follows:

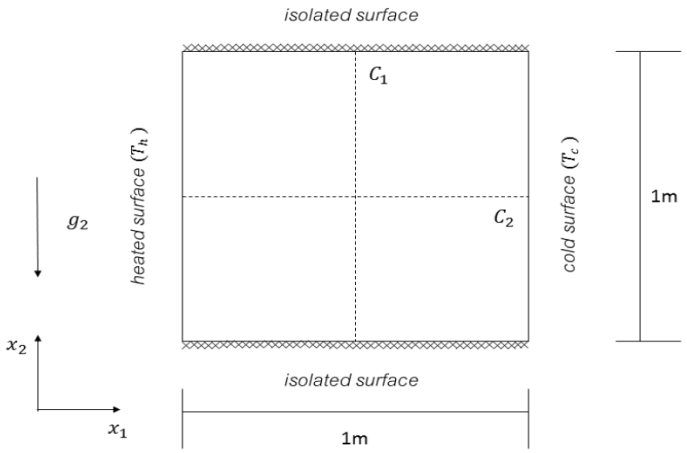

Figure 4.1: Square cavity with vertical surfaces with different temperatures.

The properties adopted for the air inside the cavity at $10°C$ are summarized bellow:

$$\begin{cases} \rho_{ref} = 1.246,6\, kg/m^-3, \\ \mu = 1.72 * 10^-5\, kgm^-1s^-1, \\ k = 2.42 * 10^-2\, Wm^-1°C^-1, \\ c_p = 1.012\, JKg^-1°C^-1, \\ M_g = 0.02896\, kg/m^3, \\ g = -9.8\, m/s^2, \\ T_{ref} = 10°C. \end{cases} \tag{4.1}$$

The mesh used was orthogonal and quadrilateral with 10.000 control volumes. For the *Fluent* program the mesh had also an orthogonal, mapped grid with the same number of control volumes. For the example, the temperature of the left wall was of $20°C$, while the temperature of the right wall was of $0°C$. The time interval used in the simulation was of 0.05 seconds and the averaged values were taken after 250 seconds (total time of compilation).

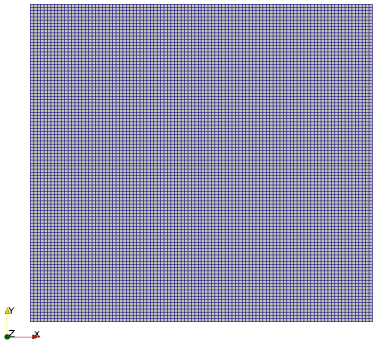

Figure 4.2: Square Cavity Mesh - 10000 quadrilaterals

The Rayleigh number, Ra, quantifies the relative magnitude of thermal driving to dissipative forces in the fluid motion, and is associated with buoyancy driven flow, also known as natural or free convection. It is defined as the product of the Grashof number, Gr, which describes the relationship between buoyancy and viscosity within a fluid, and the Prandtl number, Pr, which describes the relationship between momentum diffusivity and thermal diffusivity. For free convection near a vertical wall Ra is described as:

$$\mathrm{Ra} = \frac{Gr}{Pr} = \frac{g\,\beta\,c_p\,\rho_{ref}^2\,L^3\,|T_h - T_c|}{\mu\,k}, \tag{4.2}$$

where:

g is the acceleration due to gravity;
β is the thermal expansion coefficient;
c_p is the specific heat;
ρ_{ref} is the fluids reference density;
L is the distance between hot and cold surfaces;
T_h is the temperature of the heated surface;
T_c is the temperature of the cold surface;
μ is the dynamic viscosity;
k is the thermal conductivity.

The Grashof number for vertical flat plates is calculated as follows:

$$Gr = \frac{g\beta(T_s - T_\infty)L^3}{\nu^2}, \tag{4.3}$$

where:

T_s is the surface temperature; T_∞ is the bulk temperature.

The Prandtl number was already described in 3.14

Simulations demonstrate that for a square cavity, with vertical heated walls, laminar flows exhibit isotherm curves in some way parallel to the heated surface. That behavior corresponds to Ra around 10^4. As the Reynolds number increase, it is possible to verify that the isotherms change preferred orientation. The critical Ra for engineering purposes is situated somewhere around 10^6 and 10^8. This behavior is described as the scheme bellow.

Figure 4.3: Isotherm for Ra around 10^4

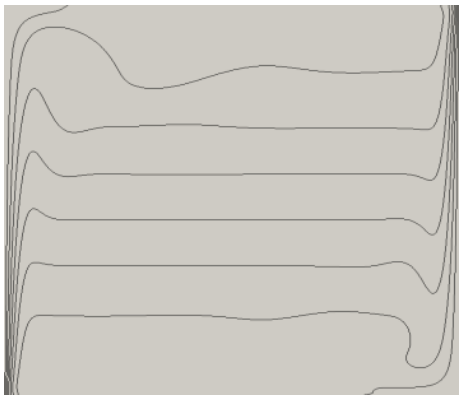

Figure 4.4: Isotherm for Ra around 10^7

The corresponding Rayleigh number calculated for the present work (4.2) was of the order of 10^9, characterizing a turbulent regime.

4.2 Achieved Results

In order to compare the results obtained from the implemented model and *Fluent*, after the total simulation time of 250 seconds, the average was considered to evaluate both models for the Rayleigh number of the order of 10^9. Temperatures were plotted along vertical and horizontal lines, $C1$ and $C2$, respectively.

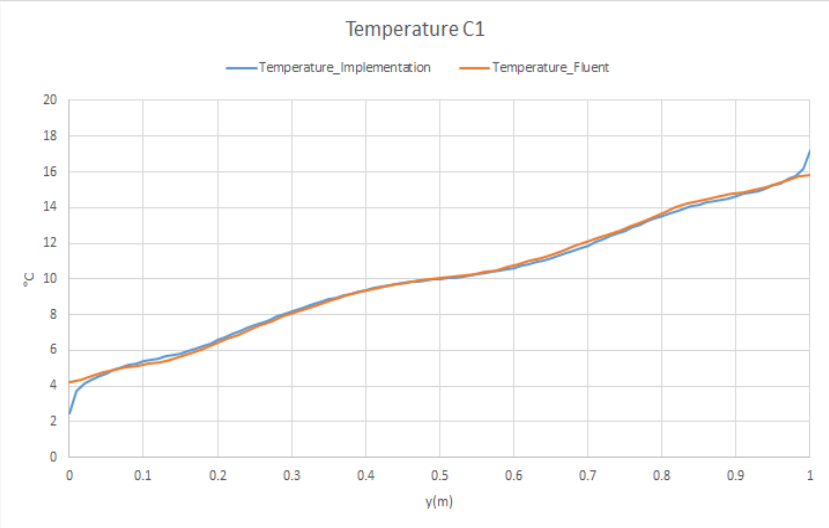

Figure 4.5: Square cavity with vertical surfaces maintained at different temperatures: Comparison of implemented model and *Fluent*'s model - Averaged temperature along the line C1 for R number of order 10^9

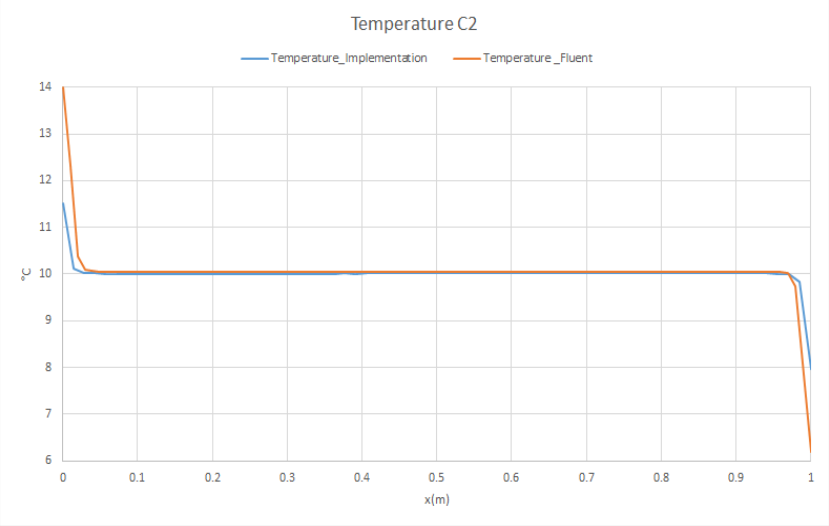

Figure 4.6: Square cavity with vertical surfaces maintained at different temperatures: Comparison of implemented model and *Fluent*'s model - Averaged temperature along the line C2 for Ra number of order 10^9

From the above figures, along line C1 (figure 4.5) it is possible to identify a slightly difference among the implemented model and *Fluent*'s model, between

vertical coordinates from 0,2 m to 0,8 m. From the central part to the top, the temperature increases, while from the central part to the bottom, the temperature decreases. Close to the walls, a difference is observed.

A way to try to control this difference could be to refine the mesh of the implemented model.

Along line $C2$ (figure 4.6) the implemented model is pretty close to *Fluent*'s model except close to the walls. The reason why temperature responds more consistently along line $C2$ than along line $C1$ is probably because of the temperature gradient that occurs in the horizontal direction (from the heated wall to the cold wall) and the movement happens in the clockwise direction, as expected.

The same averaging process was used to evaluate and compare velocity profiles between the two models for Ra of the order of 10^9 as is showed in the following figures:

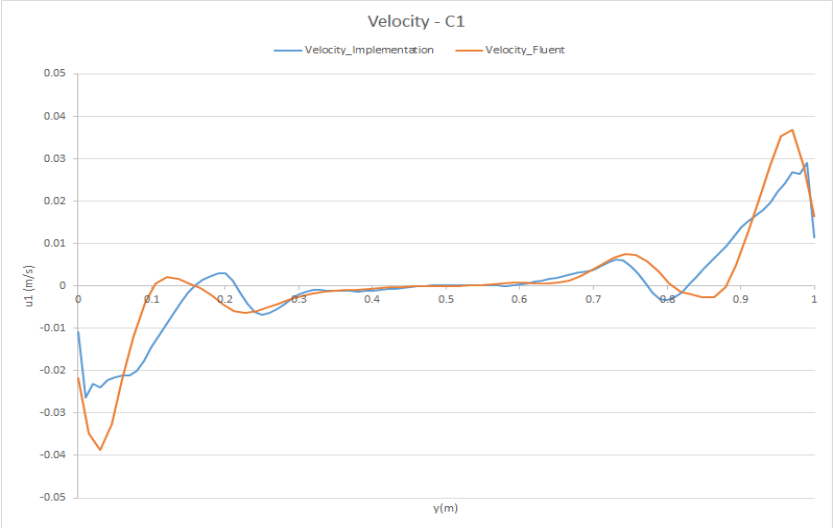

Figure 4.7: Square cavity with vertical surfaces maintained at different temperatures: Comparison of the implemented model and *Fluent's* model - horizontal velocity along the C1 line to Ra number equal to 10^9.

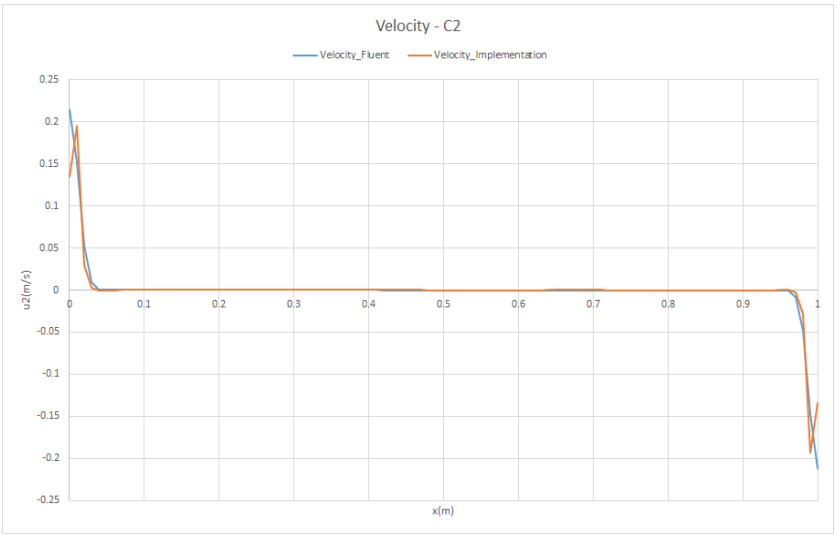

Figure 4.8: Square cavity with vertical surfaces maintained at different temperatures: Comparison of the implemented model and *Fluent*'s model - horizontal velocity along the C2 line to Ra number equal to 10^9.

The above figure shows the averaged velocities plotted, respectively, along lines $C1$ and $C2$. In figure 4.7, it can be seen that around vertical coordinates between 0.4 m and 0.6 m the models get pretty close results. Just after those points, instead, the models show differences, more sharply next to the walls. In figure 4.8, along line $C2$ the velocity shows discrepancy between models only close to the walls.

The following figures show the results obtained for the eddy viscosity in both models. The quality of the results is intrinsically related to the analysis of the velocity profile obtained in figures 4.7 and 4.8. It is clear that, close to the walls a discrepancy persists, even though it can be analyzed that for both figures 4.9 and 4.10, the expected behavior, for which close to walls the values assumed should go to zero, is achieved.

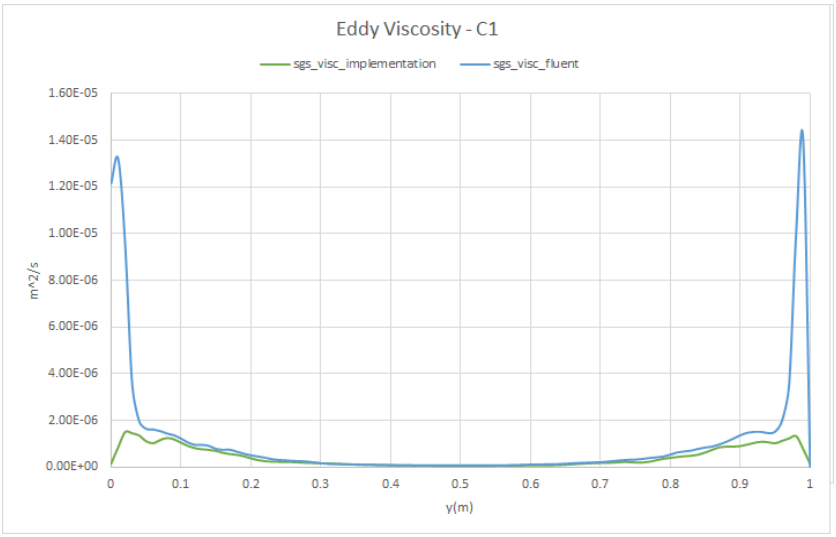

Figure 4.9: Square cavity with vertical surfaces maintained at different temperatures: Comparison of the implemented model and Fluent's model - vertical eddy viscosity along the C1 line to Ra number equal to 10^9.

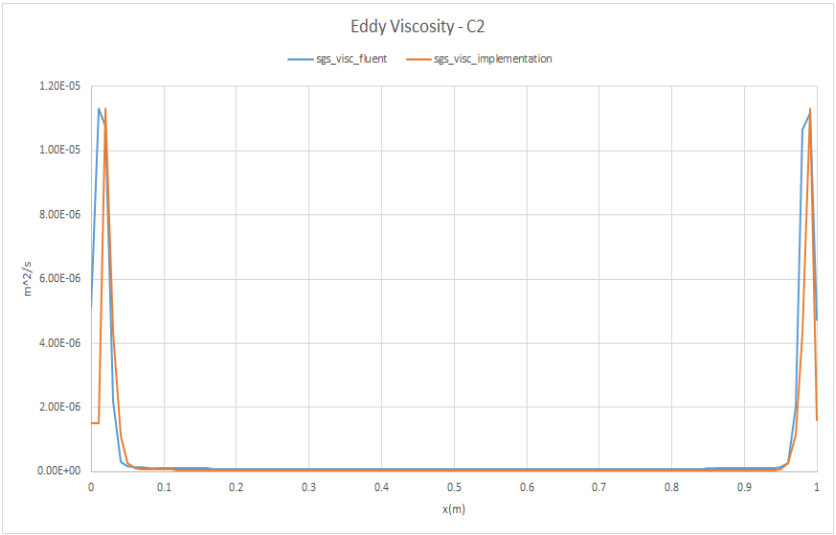

Figure 4.10: Square cavity with vertical surfaces maintained at different temperatures: Comparison of the implemented model and Fluent's model - horizontal eddy viscosity along the C2 line to Ra number equal to 10^9.

4.2.1 Conclusion

After all the studies to support this work, some considerations on the turbulence modeling phenomenon and its features can be highlighted. A turbulence model is used to give a statistically coherent response to the structure that is being analyzed. The easiest procedure used to analyze the models response are statistical procedures, being time average the simplest one. Some caution must be taken to ensure the

accuracy of the results. The flow must become fully developed, maintaining its boundary conditions. A way to do it is by increasing simulation time and checking whether the average converges to the value previously obtained.

For the implemented model the simulation time of 250 seconds was enough to evaluate the flow, since longer simulation time was tested to verify the evolution of a fully developed behavior. The model was able to handle $2D$ flow, for slightly compressible fluid flow, with meshes of quadrilaterals. The results obtained, showed that the treatment given to the walls was different between the implementation and the software Fluent. Not only for the velocity fields but also for the eddy viscosity, it is clear that the damping caused by the use of the wall function (the Van Driest function) for the implementation, was responsible for the difference between the results. By using the Van Driest function the implementation have guaranteed that the results in the wall converged to zero. Trying to activate Van Driest damping function on the Smagorinsky model, in Fluent, is a good way to confirm the results obtained in the implementation. Another valid attempt is to refine the region close to the walls and make sure that the mesh is able to resolve all the small turbulent scales within that region.

Since turbulence theory is not closed, researches and scientists are still not satisfied, because of that, many advanced studies are still being developed and implemented. To validate turbulent results, it is important to evaluate different models to make sure that the physics of the problem is being respected.

Two advanced models are interesting to be implemented and tested to verify the convergence of the values obtained for the walls. One is called Wall Adapting Local Eddy Viscosity Model - WALE, where the eddy viscosity counts with a constant of specific value $C_w = 0.325$, different from the Smagorinsky constant that assumes different values depending on the the fluid considered. Another advantage over the Smagorinsky model for the WALE model is that it returns a zero turbulent viscosity for laminar shear flow, allowing the correct treatment of linear zones in the domain. The other interesting model is the Algebraic Wall-Modeled LES - WMLES, its formulation combines a mixing length model with a modified Smagorinsky model and its advantage is that it can be combined with different models depending on the flow simulation that is being considered.For future works I would also suggest the extension of the present work for $3D$ problems.

Chapter 5

Bibliography

BALL, P., 1999, "Transitions still to be made", *Nature*, v. 402, pp. C73–C76.

BARDINA, J., HUANG, P., COAKLEY, T., 1997, "Turbulence modeling validation", *AIAA paper*, v. 2121, pp. 1997.

BOUSSINESQ, J. V., 1871, "Théorie générale des mouvements qui sont propagés dans un canal rectangulaire horizontal", *CR Acad. Sci. Paris*, v. 73, pp. 256–260.

CARVALHO, H., 2014, *O Metodo dos volumes finitos aplicado a escoamentos de conveccao forcada e natural.*

CLARK, T. L., 1977, "A small-scale dynamic model using a terrain-following coordinate transformation", *Journal of Computational Physics*, v. 24, n. 2, pp. 186–215.

DEARDORFF, J. W., 1970, "A numerical study of three-dimensional turbulent channel flow at large Reynolds numbers", *Journal of Fluid Mechanics*, v. 41, n. 02, pp. 453–480.

EULER, L., 1748, *Introductio in analysin infinitorum, auctore Leonhardo Eulero...* apud Marcum-Michaelem Bousquet.

FERZIGER, J. H., 1985, "Large eddy simulation: its role in turbulence research". In: *Theoretical approaches to turbulence*, Springer, pp. 51–72.

GERMANO, M., PIOMELLI, U., MOIN, P., et al., 1991, "A dynamic subgrid-scale eddy viscosity model", *Physics of Fluids A: Fluid Dynamics (1989-1993)*, v. 3, n. 7, pp. 1760–1765.

HEISENBERG, W., 1958. "Physics and philosophy". .

KOLMOGOROV, A. N., 1941, "The local structure of turbulence in incompressible viscous fluid for very large Reynolds numbers". In: *Dokl. Akad. Nauk SSSR*, v. 30, pp. 299–303.

LEONARD, A., 1997, "Large-eddy simulation of chaotic convection and beyond", *AIAA paper*, v. 97, pp. 0204.

LILLY, D. K., 1992, "A proposed modification of the Germano subgrid-scale closure method", *Physics of Fluids A: Fluid Dynamics (1989-1993)*, v. 4, n. 3, pp. 633–635.

NAVIER, C., 1823, "Mémoire sur les lois du mouvement des fluides", *Mémoires de lâAcadémie Royale des Sciences de lâInstitut de France*, v. 6, pp. 389–440.

POPE, S. B., 2000, *Turbulent flows*. Cambridge university press.

PRANDTL, L., 1963, *The essentials of fluid dynamics*. Blackie & Son Limited.

REYNOLDS, O., 1883, "Ph 1", *Trans. R. Soc. London*, v. 174, pp. 935.

SHAANAN, S., FERZIGER, J., REYNOLDS, W., 1975, "Numerical simulation of turbulence in the presence of shear", .

SMAGORINSKY, J., 1963, "General circulation experiments with the primitive equations: I. the basic experiment*", *Monthly weather review*, v. 91, n. 3, pp. 99–164.

STOKES, G. G., 1851, *On the effect of the internal friction of fluids on the motion of pendulums*, v. 9. Pitt Press.

VAN DRIEST, E. R., 2012, "On turbulent flow near a wall", *Journal of the Aeronautical Sciences (Institute of the Aeronautical Sciences)*, v. 23, n. 11.

VERSTEEG, H. K., MALALASEKERA, W., 2007, *An introduction to computational fluid dynamics: the finite volume method*. Pearson Education.

WERNER, H., WENGLE, H., 1993, "Large-eddy simulation of turbulent flow over and around a cube in a plate channel". In: *Turbulent Shear Flows 8*, Springer, pp. 155–168.

YEOH, G., YEUN, K., 2009. "Computation fluid dynamics in fire engineering". .